Microincapsulazione di farmaci in biopolimeri mediante atomizzazione assistita da ultrasuoni

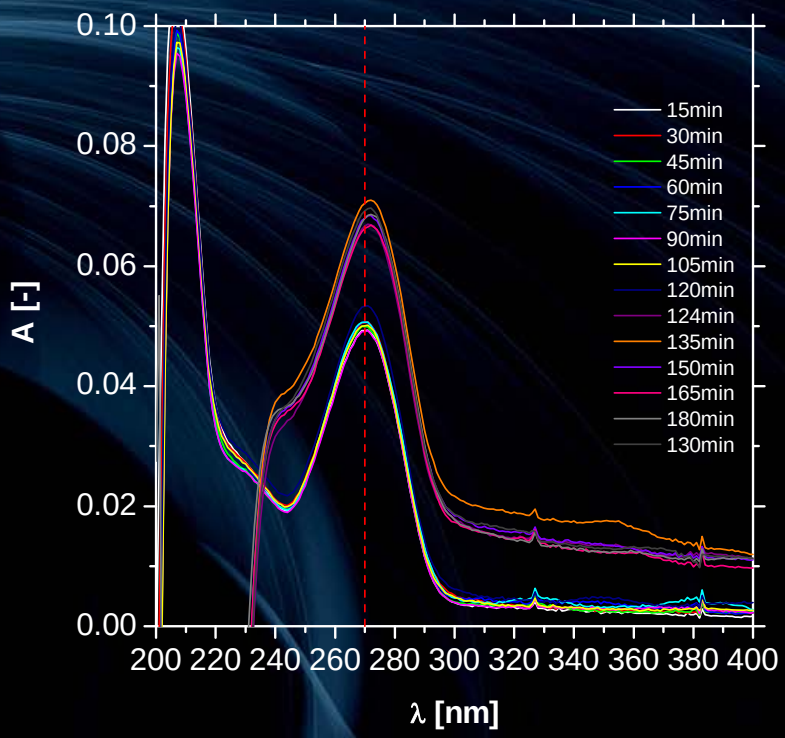

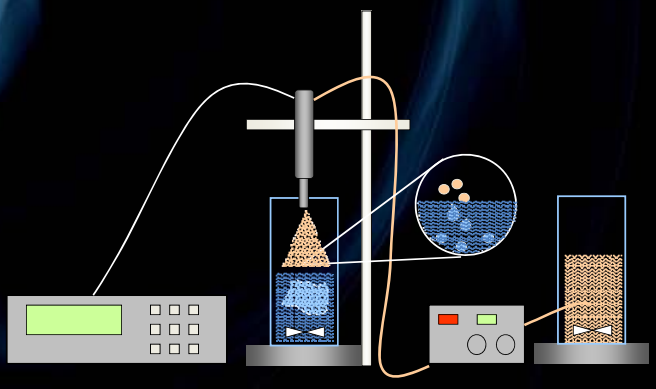

Sara Cascone

Microincapsulazione di farmaci in biopolimeri mediante atomizzazione assistita da ultrasuoni
Sara Cascone

UNIVERSITÀ DEGLI STUDI DI SALERNO

Facoltà di Ingegneria

Corso di Laurea in Ingegneria Chimica

Microincapsulazione di farmaci in biopolimeri mediante atomizzazione assistita da ultrasuoni

Tesi in
Principi di Ingegneria Chimica

Relatori:

Prof. Ing. Giuseppe Titomanlio

Prof. Ing. Gaetano Lamberti

Candidata:

Sara Cascone

Matricola 0620200095

Anno Accademico 2008/2009

Una cornacchia, mezza morta di sete, trovò una brocca che una volta era stata piena d'acqua. Ma quando infilò il becco nella brocca si accorse che vi era rimasto soltanto un po' d'acqua sul fondo. Provò e riprovò, ma inutilmente, e alla fine fu presa da disperazione. Le venne un'idea e, preso un sasso, lo gettò nella brocca.

Poi prese un altro sasso e lo gettò nella brocca.
Ne prese un altro e gettò anche questo nella brocca.

Piano piano vide l'acqua salire verso di sé, e dopo aver gettati altri sassi riuscì a bere e a salvare la sua vita.

"A poco a poco si arriva a tutto."

Questo testo è stato stampato in proprio, in Times New Roman

La data prevista per la discussione della tesi è il 20.11.09
Fisciano, 16.11.09

Sommario

Indice delle figure

Indice delle tabelle

Lista delle pubblicazioni

Lista delle pubblicazioni

Barba, A.A.; d'Amore, M.; **Cascone, S.**; Chirico, S.; Lamberti, G.; Titomanlio, G. "On the behavior of HPMC/theophylline matrices for controlled drug delivery", Journal of Pharmaceutical Sciences, 98(11) 4100-4110 (2009), doi: 10.1002/jps.21701, IF 2008: 2.996.

Barba, A.A.; d'Amore, M.; **Cascone, S.**; Lamberti, G.; Titomanlio, G. "Intensification of biopolymeric microparticles production by ultrasonic assisted atomization", Chemical Engineering and Processing: Process Intensification, 48(10) 1475-1481 (2009), doi: 10.1016/j.cep.2009.08.004, IF 2008: 1.518.

Cascone, S.; Chirico, S.; Lamberti, G.; Titomanlio, G. "Water and theopylline transport phenomena within HPMC based tablets", Proceedings of Innovation in Drug Delivery, Napoli, 30 September - 3 October 2007.

Barba, A.A.; d'Amore, M.; **Cascone, S.**; Lamberti, G.; Titomanlio, G.; "Intensification of pharmaceuticals atomization by ultrasonic: experiments and correlations testing", GPE-EPIC 2009, 14-17 June 2009, Venice (Italy).

Barba, A.A.; **Cascone, S.**; Di Muria, M.; Lamberti, G.; "Micro-particles by ultrasonic atomization: new strategy towards novel drug carrier", CRS36, 18-22 July 2009, Copenhagen (Denmark).

Barba, A.A.; d'Amore, M.; **Cascone, S.**; Lamberti, G.; Titomanlio, G.; "Microencapsulation of nutraceuticals and pharmaceuticals by ultrasonic atomization" to be presented to Effost 2009 – Budapest, 11-13 November 2009 Hungary.

È allegata la seguente pubblicazione:

Barba, A.A.; d'Amore, M.; **Cascone, S.**; Lamberti, G.; Titomanlio, G. "Intensification of biopolymeric microparticles production by ultrasonic assisted atomization", Chemical Engineering and Processing: Process Intensification, 48(10) 1475-1481 (2009), doi: 10.1016/j.cep.2009.08.004, IF 2008: 1.518.

Chemical Engineering and Processing 48 (2009) 1475–1481

Contents lists available at ScienceDirect

Chemical Engineering and Processing: Process Intensification

journal homepage: www.elsevier.com/locate/cep

Intensification of biopolymeric microparticles production by ultrasonic assisted atomization

Anna Angela Barba [a,*], Matteo d'Amore [a], Sara Cascone [b], Gaetano Lamberti [b], Giuseppe Titomanlio [b]

[a] Dipartimento di Scienze Farmaceutiche, Università degli Studi di Salerno, Ponte don Melillo, 84084 Fisciano (SA), Italy
[b] Dipartimento di Ingegneria Chimica e Alimentare, Università degli Studi di Salerno, via Ponte don Melillo, 84084 Fisciano (SA), Italy

ARTICLE INFO

Article history:
Received 19 July 2009
Received in revised form 10 August 2009
Accepted 12 August 2009
Available online 20 August 2009

Keywords:
Intensified ultrasonic atomization
Microparticles
Biopolymer

ABSTRACT

In this work ultrasonic atomization process is applied to produce biopolymer microparticles with potential applications in pharmaceutical and nutraceutical fields. Natural polymer (alginate)/water solution is atomized by ultrasonic assisted process and the droplets spray is reticulated using a solution of copper sulfate, where the Cu^{2+} ions cause the formation of a network structure (hard porous gel). Several operating parameters (solution concentration, flow rate, atomization power) are changed to study their effects on the produced microparticles. Literature correlations able to predict the features of the droplets as functions of process parameters are optimized using a statistical approach. Furthermore, the energy requirement for the drops production is compared with the energy required by traditional techniques to evaluate the intensification effect of the ultrasonic on the atomization process.

1. Introduction

1.1. Generalities

Fine particles are widely used in the preparation of pharmaceutical dosage systems and food supplements. A very common way to get fine particles is the spray drying process, where the most important step is the atomization. In conventional atomization techniques the break-up of a liquid jet in droplets is caused by transformation or transfer of large amounts of energy (into surface energy). In the single fluid atomizers, the pressure energy is changed in kinetic energy by passing in small orifices (nozzle atomizers); or the kinetic energy is supplied by rotary parts (rotary wheel atomizers). In the two fluids atomizers, the drag force (due to the difference in kinetic energy) at the interface between the two fluids induces the formation of a thin liquid film which, in turn, is reduced in threads that, finally, give rise to fine droplets. In all these cases energy consumptions are the crucial drawbacks in the production of fine particles. Currently, many researches (on design and development of novel procedures for manufacturing fine chemicals, pharmaceuticals and foods) are performing to meet the new approach in matter of production: the process intensification (PI). Process intensification may be defined as a strategy which aims to achieve process miniaturisation, reduction in capital cost, improved inherent safety and energy efficiency, and often improved product quality. Furthermore, process intensification encompasses also intensified methods of processing which may involve the use of ultrasonic and radiation energy sources [1].

Ultrasonic atomization technique is, thus, proposed and applied as process intensification tool since it requires much less energy, with respect to conventional atomization steps, to produce droplets because it works involving low velocities. By ultrasonics droplets are achieved spreading liquids onto a surface which is vibrated at ultrasonic frequencies (ranging from 20 kHz to 30 MHz). The vibrations causes the formation of threads and then of droplets. Very small droplets can be produced by increasing the frequency and it is known that liquid feed properties (mainly surface tension and viscosity) affected the threads formation (in terms of thickness) and, in turn, the droplet size. Many literature references report analyses and hypotheses about the mechanism that explain the liquid disintegration mechanism during ultrasonic atomization. Rajan and Pandit [2] summarized historical and currently approaches to elucidated the disruption of liquid threads in droplets and discussed the two major mechanism: cavitation and capillary wave hypotheses. Cavitation phenomenon seems occurred at high both energy intensity and frequency and is based on the formation and violent collapse of small vacuum bubbles promoted by the alternating low-pressure and high-pressure waves in liquids. Capillary wave hypothesis is based on the so-called Taylor instability, i.e. the atomization occurs when instable oscillations split the peaks of surface capillary waves (capillary waves are composed by crests or peaks and troughs) away from the bulk liquid. Since the drops are produced from peaks their sizes are proportional to wavelength. This latter decreases with the increasing of ultrasonic frequency, so fine droplets are obtained at higher frequencies.

* Corresponding author. Tel.: +39 089969240; fax: +39 089969602.
E-mail address: aabarba@unisa.it (A.A. Barba).

0255-2701/$ – see front matter © 2009 Elsevier B.V. All rights reserved.
doi:10.1016/j.cep.2009.08.004

Although the principles of ultrasonic atomization are known and applied since the 1960s of the last century, a reliable correlation between operating parameters and droplet size, accounting for all the relevant physical parameters, still lacks.

1.2. Aims of this work

Aim of this work is to point out an ultrasonic atomization method, on the laboratory scale, to produce small droplets of biopolymer (alginate) intended for the preparation of encapsulated drug/nutraceutical delivery systems. The selection and the optimization of the best correlations between process parameters and the size of obtained particles are also performed and proposed.

2. Experimental

2.1. Materials

Sodium alginate (CAS number 9005-38-3, Sigma cat. W201502) and copper sulfate penta-hydrate (CAS number 7758-99-8, Sigma cat. C8027) were purchased from Sigma Aldrich s.r.l., Milano IT. Distilled water was produced by water evaporation and condensation cycle.

Alginate is a biocompatible, mucoadhesive, biodegradable and pH-responsive hydrogelic biopolymer consisting of (1→4)-O-glycosidic links of β-D-mannuronic and α-L-guluronic acid residues at varying sequential arrangements and proportions [3]. For these features it is often adopted in the formulating of pharmaceutical dosage forms [3–8], in nutraceutical products and food supplements [9–13]. Due to its ability to form ionotropic physical gel by cooperative binding with multi-valent cations (such as calcium, barium, copper), alginate is used to encapsulate in network structure drugs, therapeutic biomolecules, functional compounds such as vitamins and antioxidant.

Brandenberger and Widmer [14] report that, for a $c^* = 1.3\%$ alginate water solution, the density is $\rho^* = 1050\ kg\ m^{-3}$ and the surface tension is $\sigma^* = 55\ m\ N\ m^{-1}$. Assuming linear behavior for these two variables in the investigated concentration range [13] (the linear behavior holds up to the Critical Micellization Concentration, which for this system is higher than the investigated concentration range), the solution density and surface tension are given by

$$\rho(c) = \rho_0 + m_\rho c \quad (1)$$

$$\sigma(c) = \sigma_0 + m_\sigma c \quad (2)$$

with ρ_0 = water density = $1000\ kg\ m^{-3}$; σ_0 = water surface tension = $70.8\ m\ N\ m^{-1}$; $m_\rho = (\rho^* - \rho_0)/c^*$ and $m_\sigma = (\sigma^* - \sigma_0)/c^*$.

The viscosity of alginate solutions could be described by the power-law (which is valid for shear rates far from the Newtonian ones), i.e.

$$\eta = K\dot{\gamma}^{n-1} \quad (3)$$

The consistency index, K, and the flow index, n, are functions of the alginate concentration, c. The data given in literature [14] for concentration range between 1 and 3% are well described by the fitting equations (c in %, K in Pa s^n, n dimensionless):

$$K(c) = 0.0619c^{2.953} \quad \text{and} \quad n(c) = 0.9635\ \exp(-0.08c) \quad (4)$$

As a measure of the shear rate, the shear rate at the wall for a power-law fluid with a volumetric flow rate $\dot{V}$ flowing in a circular tube of radius R is taken [16]:

$$\dot{\gamma}_w = \left[\left(\frac{1}{n} + 3\right)\frac{\dot{V}}{\pi R^3}\right]^n \quad (5)$$

Thus, the solution viscosity has to be estimated calculating the power-law parameters by Eq. (4) (for each solution with different concentration), then the shear rate by Eq. (5) (for each run with different volumetric flow rate) and finally the viscosity by Eq. (3).

2.2. Apparatuses

The VCX 130 PB Ultrasonic Processors (130 W, 20 kHz, Sonics & Materials Inc., CT, USA) and a standard tip for low atomization rate (up to $1\ mm^3\ s^{-1}$), code VC 4020 (50 W, 20 kHz, Sonics & Materials Inc., CT, USA) were adopted as source of ultrasonic vibration and atomizer, respectively.

Also a peristaltic pump (Velp Scientifica, IT) and an optical microscope (Leica DM-LP, Leica Microsystems GmbH, Wetzlar, DE) were used for the experiments.

2.3. Software

Image analysis was performed by the public domain software ImageJ 1.40g (Wayne Rasband, National Institutes of Health, USA, the software is freely available at http://rsb.info.nih.gov/ij/). Correlation testing, regression and statistical analysis were performed by Mathcad 14 (© 2007 Parametric Technology Corporation, MA, USA).

2.4. Methods

Laboratory tests were performed by spraying the alginate solution, for small time intervals (4–5 s), into a beaker containing stirred copper sulfate solution ($20\ g\ [CuSO_4{\cdot}5H_2O]\ L^{-1}$), see Fig. 1. This value gives a fast reticulation (the formation of a rigid network characterized by the so-called "egg-box" structures, in which alginate molecules were coordinated by bivalent positive ions [3]; as has been tested during our investigation of the alginate reticulation kinetics. The alginate reticulation is a very fast reaction, which takes place immediately after the impact between the alginate drop and the copper solution. Due to the impact, the spherical drop deforms assuming a pendant shape, and if the reticulation takes place fast enough, that will keep the shape once solidified (see the inset in Fig. 1). The produced particles show a density very close to the water density, just a little higher. For each experiment, a sample of the solution obtained was observed microscopically, some snapshot were taken, and the particles produced were measured by image analysis (see an example in Fig. 2). By this way, the diameters for a number of particles (20–30 items) were obtained, and

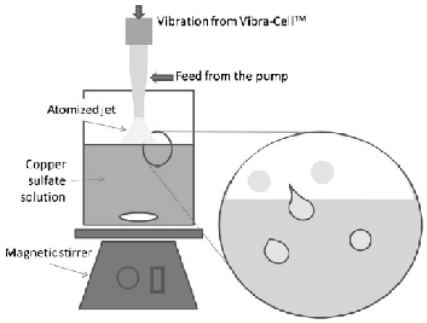

Fig. 1. Schematic of the experimental set up. In the inset: the droplet-like formation (pictorial).

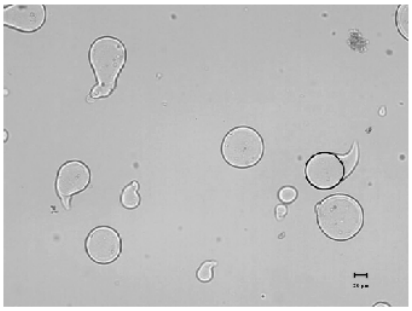

Fig. 2. Image from optical microscopy of a sample (run no. 21. $c = 2\%$, $\dot{V} = 0.252 \times 10^{-6}$ m^3 s^{-1} $P = 5.8$ W). The bar is 20 μm.

then the average diameter and the standard deviation of the data were calculated.

3. Results and discussions

A summary of all the experimental runs performed during this study is reported in Table 1. The parameters reported in the following were changed: the alginate solution concentration (1, 2 and 3% w/w), the volumetric flow rate (in the range 0.1–0.6 mm^3 s^{-1}), obtained by measuring the volume of the solution pumped during a given time interval), and the power level of the source of ultrasonic wave (in the range 4–11 W). The actual power delivered to the atomizer was a direct output of the VCX 130 PB (Ultrasonic Processor), in term of the ratio of the total energy over the time. In Table 1, for each run, the average diameter obtained from image analysis was reported, along with observed standard deviation of data.

For each alginate solution concentration, four different levels of volumetric flow rate were investigated. The flow rate is practically the same for each concentration. Thus, the minimum flow rate is 0.137 mm^3 s^{-1} for 1% solution, and it is 0.136 mm^3 s^{-1} for 2% solution and it is 0.139 mm^3 s^{-1} for 3% solution. The second level is around 0.26 mm^3 s^{-1}, the third level around 0.40 mm^3 s^{-1}, and the fourth level around 0.55 mm^3 s^{-1}. For each couple (concentration, flow rate) at least three different power levels were tested. Within the first series (1%, 0.137 mm^3 s^{-1}, test #1–8), some tests have been repeated with the same power level to assess the method reliability (see tests 3 and 4 as well as tests 6 and 7). Obtaining the same particle average diameter, the repeatability of the experiments has been confirmed. For example, tests 3 and 4 gives average diameters of 58.14 and 58.43 μm, respectively, then the difference (roughly 0.3 μm) is well below the standard deviation of the data (11.3 and 14.6 μm).

Some trends clearly emerge from the set of experiments performed (even if some of the observed trends fall within the experimental error of the method):

1. The particle diameter *decreases* (a little) with the level of the *power delivered* – see each series of data in which the only varying parameter is the power delivered, e.g. tests #9–10–11 or tests #36–37–38.
2. The particle diameter *increases* with the *volumetric flow rate*, see for example the series of runs #5–10–15 (which are at similar power levels, not exactly the same).
3. The particle diameter *increases* with the *alginate concentration* (this observation requires some interpolations, see for example tests # 13/14–26–36/37).

Of course, the number of the parameters involved is very high (viscosity, viscosity dependence upon shear rate, surface tension, and density of the solution, frequency and amplitude of the sonic wave, flow rate, delivered power). Thus the most effective way to approach to the problem is the dimensional analysis, the final goal being a correlation able to predict the particle diameter as a function of the process parameters.

3.1. Correlations testing

The first correlation proposed to predict the diameter produced by ultrasonic atomization (at the frequency f) is the one due to Lang [17]:

$$D_L = 0.34\left(\frac{8\pi\sigma}{\rho f^2}\right)^{0.33} \tag{6}$$

The Lang equation is really simple, but it does not account for the following process parameters: solution flow rate and delivered

Table 1
Measured average diameters, D, along with their standard deviations, SD, as function of: alginate solution concentration, c; mass flow rate, $\dot{V}$; and atomization power, P.

$c = 1\%$				$c = 2\%$				$c = 3\%$			
#	$\dot{V}$ (mm^3 s^{-1})	P (W)	$D \pm$ SD (μm)	#	$\dot{V}$ (mm^3 s^{-1})	P (W)	$D \pm$ SD (μm)	#	$\dot{V}$ (mm^3 s^{-1})	P (W)	$D \pm$ SD (μm)
1	0.137	5.200	58.09 ± 8.88	18	0.136	6.257	86.32 ± 15.05	30	0.139	7.556	93.96 ± 16.34
2	0.137	5.545	58.87 ± 10.43	19	0.136	6.364	90.8 ± 28.55	31	0.139	7.882	93.63 ± 18.48
3	0.137	6.333	58.14 ± 11.32	20	0.136	9.900	83.16 ± 11.62	32	0.139	10.887	82.46 ± 19.33
4	0.137	6.333	58.43 ± 14.6								
5	0.137	7.133	60.84 ± 20.53								
6	0.137	8.333	58.09 ± 16.34								
7	0.137	8.364	58.58 ± 12.63								
8	0.137	8.600	60.56 ± 15.89								
9	0.256	4.167	64.17 ± 6.9	21	0.252	5.818	90.79 ± 20.1	33	0.256	7.308	95.8 ± 35.25
10	0.256	7.000	61.6 ± 15.89	22	0.252	6.182	88.95 ± 19.3	34	0.256	8.417	74.73 ± 27.25
11	0.256	8.125	59.51 ± 21.24	23	0.252	9.375	87.65 ± 22.76	35	0.256	9.500	70.63 ± 16.68
12	0.44	6.143	68.3 ± 10.48	24	0.396	6.111	104.31 ± 25.08	36	0.366	8.083	107.01 ± 28.02
13	0.44	6.714	67.81 ± 20.53	25	0.396	8.833	110.25 ± 26.33	37	0.366	9.000	104.8 ± 29.12
14	0.44	9.571	64.92 ± 11.3	26	0.396	8.875	92.32 ± 21.04	38	0.366	9.750	84.3 ± 19.26
15	0.593	6.875	75.07 ± 16.72	27	0.518	6.286	104.24 ± 24.25				
16	0.593	8.000	71.25 ± 21.31	28	0.518	6.800	101.95 ± 23.49				
17	0.593	8.900	68.85 ± 10.12	29	0.518	9.286	103.03 ± 25.88				

power, as well as for the material parameter describing the solution viscosity. On the contrary, all of these three parameters were proven to be very important in ultrasonic atomization. In the conditions of present work, the diameters predicted by Lang's equation ⟨G⟩ are 52, 47 and 42 μm, respectively, for c = 1, 2 and 3% (changes in alginate concentration causes changes of density and surface tension of the solutions). Inspection of Table 1 confirms that the predictions of Lang's equation are far from the experimental values and that the complex behavior depicted by experimental data cannot be predicted by that equation, Eq. (6).

In a very detailed paper, Rajan and Pandit [2] proposed two different approaches to predict the droplet diameter. In the first one a correlation was developed in term of "perturbation" of the Lang's equation. The coefficient 0.34 in Lang's equation was replaced by a function of some dimensionless parameters:

$$D_A = \left(\frac{\pi\sigma}{\rho f^2}\right)^{0.33} [1 + P_1 We^{P_2} Oh^{P_3} In^{P_4}] \tag{7}$$

In the correlation (7), which is named "Correlation A" in the present work, the dimensionless parameters are:

- the modified Weber number,

$$We = \frac{f\dot{V}\rho}{\sigma} \tag{8}$$

- the Ohnesorge number,

$$Oh = \frac{\eta}{fAm^2\rho} \tag{9}$$

- the Intensity number,

$$In = \frac{f^2 Am^2}{CV} \tag{10}$$

In these equations, C is the speed of sound, Am is the amplitude of the sound wave and the other symbols have been already defined. The amplitude Am can be evaluated as

$$Am = \frac{1}{2\pi f}\sqrt{\frac{2I}{\rho C}} \tag{11}$$

where $I = P/A$ is the power surface intensity. It is calculated as the ratio between the power delivered and the surface of the ultrasonic actuator. The values for parameters P_1–P_4 proposed by [2] were reported in Table 2, in the section for Correlation A, the column named "Not optimized".

A large experimental campaign was carried out by Rajan and Pandit [2] to test the correlations found in literature, including their own equation (7). Correlation A. They varied the volumetric flow rate, the delivered power, the surface tension by varying the sodium lauryl sulfate concentration in water, the viscosity by varying the percentage of glycerine added to their solutions and the density by varying the amount of sodium chloride added to their solutions. The high number of experimental data available allowed to regress the dependence of the drop diameter from each single variable. Thus, they proposed a further correlation directly in term of governing variables, with the structure:

$$D_B = P_1 f^{P_2} \dot{V}^{P_3} \sigma^{P_5} \rho^{P_5} \eta^{P_6} I^{P_7} \tag{12}$$

In Eq. (12), which is named "Correlation B" in the present work, all the variables were already known. The values for parameters P_1–P_7 proposed by [2] were reported in Table 2, in the section for Correlation B, the column named "Not optimized". By using these values, the Correlation B gives the diameters in micrometer ([2] reports P_1 = 1600 and the diameters are in meter).

Rajan and Pandit [2] tested these two correlations by comparison with experimental data obtained working with solutions of sodium lauryl sulfate, glycerine and NaCl. The physical properties and the operating conditions were very similar to the one obtained in the present work. The authors themselves confirmed the inadequacy of Correlation A (Eq. (7)) in describing their experimental data. They also stated that Correlation B (Eq. (12)) with the parameters obtained by fitting the effect of each single process variable (density, viscosity, surface tension, flow rate, power delivered, ultrasonic frequency) was better but not enough so they concluded that "a further improvement can be made by optimizing the exponents".

Along with the present experimentation, the cylindrical surface of the actuator is $A = 2\pi R_{act} L_{act} = 4.34 \times 10^{-4}$ m^2 (being R_{act} = 1.15 mm and L_{act} = 60 mm), f = ultrasonic frequency = 20 kHz and C = speed of sound (in the water) = 1497 m s^{-1}. With these values, and the data of Table 1, both the correlations, A and B, can be applied to the runs performed, to test their reliability.

Fig. 3 is a parity plot which summarizes all the runs performed. The abscissas are the measured diameter and the ordinates are the calculated diameters. A correlation is able to predict the right diameter if the points in such a plot falls on the diagonal (which is drawn as a continuous line). The predictions reported in Fig. 3 have been obtained by Correlation A (Eq. (7)) and B (Eq. (12)), with the parameters given in literature and reported in Table 2. It is evident that, even if Correlation B is a little better, no one of the two correlations is able to predict the observed data. The inadequacy of the two correlations is further confirmed by the statistical analysis, which results were reported in Table 2, too. The Sum of Square Errors (SSE) is very high for both the correlations (the order of 10^5 μm^2), the Pearson coefficient, R^2, is far from unity, the average diameters, $\langle D_A \rangle$ = 243.1 μm and $\langle D_B \rangle$ = 153.9 μm, are both very far from

Table 2
Statistical analysis for correlations testing. For experimental data: N = 48 points, $\langle D \rangle$ = 79.4 μm and VAR = 288.1 μm^2.

	Correlation A			Correlation B	
	Non-optimized	Strategy 1	Strategy 2	Non-optimized	Strategy 1
P_1	0.100	0.160	8.21×10^7	1600	1.737
P_2	0.220	1.003	0.977	−0.600	−0.290
P_3	0.166	0.725	0.811	0.267	0.162
P_4	−0.0277	0.406	−0.015	0.110	0.106
P_5				−0.274	−0.228
P_6				0.166	0.187
P_7				−0.400	−0.243
SSE (μm^2)	10.20×10^5	7.03×10^3	7.11×10^3	2.26×10^5	2.25×10^3
R^2	0.727	0.374	0.469	0.737	0.789
$\langle D \rangle$ (μm)	243.1	83.9	84.7	153.9	78.5
VAR (μm^2)	869.9	47.1	72.7	741.6	225.3
t-Test on $\langle D \rangle$	Fail	OK	OK	Fail	OK
χ^2-Test on VAR	Fail	Fail	OK	Fail	OK

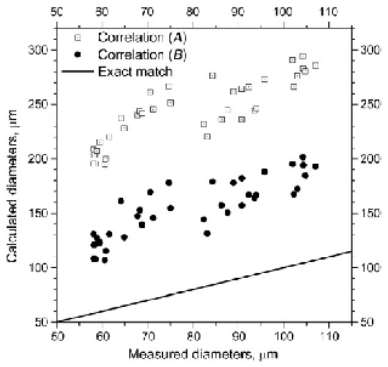

Fig. 3. Calculated diameters vs. measured diameters, before the optimization. Open squares: correlation (*A*), full circles: correlation (*B*), continuous line: the exact match ($D_{calc} = D_{meas}$).

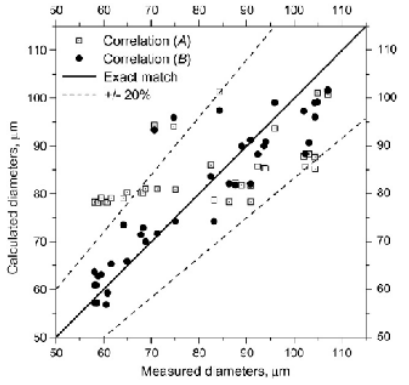

Fig. 4. Calculated diameters vs. measured diameters, after the optimization (Strategy 1 for both the correlations, see the text). Open squares: correlation (*A*), full circles: correlation (*B*), continuous line: the exact match ($D_{calc} = D_{meas}$), dashed lines: −20% from exact march.

experimental one, $\langle D \rangle = 79.4$ μm. Similarly, the variance of the two predicted sets of data, $VAR_A = 869.9$ μm^2 and $VAR_B = 741.6$ μm^2, are both very different from the experimental one, VAR = 288.1 μm^2. Even if it is evident, the statistical significance of the data was tested by the *t*-test on the average diameters and by the χ-squared test on variance. All of these tests of course failed.

Since the two correlations reveal themselves inadequate to predict the particle diameter for the investigated system, an optimization procedure has been performed to make them useful for the diameters calculation. During a first optimization (Strategy 1), the Correlation *A* was optimized letting all the parameters but P_1 to vary (i.e. the parameter P_1 was kept constant on its value taken from literature, 0.1), whereas for Correlation *B* all the parameters were allowed to vary. The optimization procedure consists in searching the values for parameters which minimize the SSE. The search was carried out by the built-in Mathcad's command based on Levenberg and Marquardt technique. Results of the first strategy were reported both in Table 2 (columns named "Strategy 1") and in Fig. 4 (parity plot).

It is evident from Fig. 4 that Correlation *A* optimized following Strategy 1 (i.e. allowing to vary all the parameters but P_1), even if it performs much better than prior of the optimization, still is insufficient for predictive purposes. Indeed, the processes carried out under conditions which produce lower diameters (low flow rate, low alginate concentration) were not rightly described, leading to predicted diameters larger than the experimental ones. On the other hand, Correlation *B*, once optimized (i.e. using the parameters listed in the last column of Table 2), predicts the diameter satisfactorily, since the data points reported in Fig. 4 were close to the parity line (the diagonal), and all data but two falls in a region within the 20% from the diagonal (the region identified by the two dashed lines). Of course, these considerations were supported by the statistical analysis (all the values mentioned in the following are reported in Table 2). For both the optimized correlations, the Sum of Square Errors were considerably reduced (from 10^5 to 10^3) and the predicted average diameters were much closer to the experimental ones ($\langle D_A \rangle = 83.9$ μm and $\langle D_B \rangle = 79.5$ μm, while the experimental one is $\langle D \rangle = 79.4$ μm). Therefore, both the correlations pass the *t*-test on the average diameter (which means that both the correlations were able to predict the average of the set of experimental diameters). However, for optimized Correlation *A* the statistical analysis does not allow to take the correlation as a predictive tool. Indeed, the Pearson coefficient is very low (less than 0.4), and the variance is very different from the experimental one ($VAR_A = 47.1$ μm^2, while the experimental one is VAR = 288.1 μm^2), thus the χ-squared test on variance was failed. Therefore, one can conclude that the Correlation *A*, even after optimized performed following Strategy 1, was not suitable for prediction purposes. On the other hand, for optimized Correlation *B* both the Pearson coefficient (around 0.8) and the variance ($VAR_B = 226.3$ μm^2, while the experimental one is VAR = 288.1 μm^2, Correlation *B* thus passes also the χ-squared test on variance) confirm the goodness of the predictions.

Thus, a different strategy optimization was followed, limited to the Correlation *A*. In Strategy 2 all the parameters were let to be changing. The optimizer causes the parameter P_1 assuming a very low level (close to 0), and the results of this step were summarized in Table 2 (column named "Strategy 2") and in Fig. 5 (only the symbols for Correlation *A* were changed with respect to Fig. 4). The predictions were a little bit better, as shown by the graph (the lower diameters still are unpredictable) and confirmed by the statistical data. The SSE reduced a little with respect to Strategy 1, Correlation *A*, but it remains more than three times the value obtained by Correlation *B*. The average diameter is reasonable and the variance increases a little with respect to Strategy 1, thus the Correlation *A* now (barely) passes both *t*-test and the χ-squared tests. However, the Pearson coefficient still is unacceptable (less than 0.5). In conclusion, the Correlation *A* reveals itself of no use in diameter prediction for the investigated system.

One last consideration has to be carried out in the selection of the correlation to be used in diameter prediction. Does the increase in prediction quality deserve the increase in parameters number, since the Correlation *A* requires 4 parameters and Correlation *B* requires 7 parameters? To answer to this question, a test has been performed following the Akaike Information Criterion [18], for which the value $\Delta AIC = n \ln(SSE_2/SSE_1) + 2\Delta\pi$ has to be evaluated, in which n is the number of data points (here $n = 38$). SSE are the Sum of Square Errors for the model-1, the one with less parameters (Correlation *A*, optimized following the Strategy 2 which is the best) and for the model-2, the one with more parameters (optimized Correlation *B*), $\Delta\pi$ is the difference between the number of

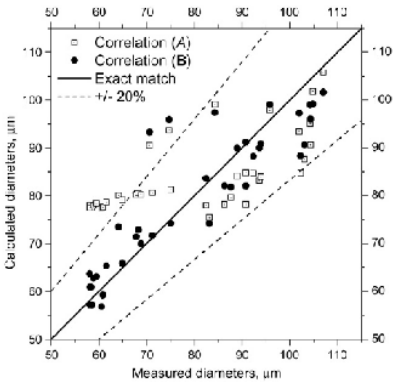

Fig. 5. Calculated diameters vs. measured diameters, after the optimization (*Strategy 2 for Correlation A. Strategy 1 for Correlation B, see the text*). Open squares: correlation (A), full circles: correlation (B), continuous line: the exact match ($D_{calc}=D_{meas}$), dashed lines: +20% from exact match.

parameters for the two models (here $\Delta\pi = 7 - 4 = 3$). If the difference in AIC is positive, then the change in sum-of-squares (the first term, always negative) is not as large as expected from the change in number of parameters (the second term, always positive), so the simpler model is more likely to be correct. In the present case, $\Delta AIC = -39.1 < 0$, thus the use of the Correlation *B* is statistically justified.

The two approaches given by Eqs. (7) and (12), Correlations *A* and *B*, respectively, were both suggested by [2]. The statistical analysis carried out in the previous paragraph showed the inefficiency of Correlation *A* (Eq. (7)) in describing our data. Correlation *B* (Eq. (12)) was found able to reproduce the experimental data with good accuracy. However, Eq. (12) is a dimensional equation, relating seven different variables ($D, f, \dot{V}, \sigma, \rho, \eta, I$) which can be expressed in term of three different primary dimensions (length, mass, time). Then, dimensional analysis states that equation (12) can be reduced to a correlation between four (seven variables minus three primary dimensions) dimensionless parameters. For example, the relationship could be expressed as

$$D = \Pi_1 \left(\frac{\pi\sigma}{\rho f^2}\right)^{0.33} We^{\Pi_2} Oh^{\Pi_3} In^{\Pi_4} \qquad (13)$$

The above equation with proper values for the four parameters $\Pi_1 - \Pi_4$, gives exactly the same predictions of Eq. (12), using three parameters instead of seven. The values of these four parameters are: $\Pi_1 = 0.058$, $\Pi_2 = 0.151$, $\Pi_3 = 0.192$, $\Pi_4 = -0.020$.

The meaning of Eq. (13), along with the parameters obtained by fitting, is that the average particle size increases if Weber and Ohnesorge numbers increase, and decreases if Intensity number increases. An increase in Weber number (which is given by Eq. (8)) means that the mass flow rate is increased or that the surface tension is decreased. However such kind of analysis should be carefully carried out: indeed, spraying a fluid which has a low surface tension will increase the Weber number (which contains $\sigma^{-\Pi 2} = \sigma^{-0.151}$) but in the multiplying factor there is $\sigma^{0.33}$, thus the final effect of a decrease in surface tension is a decrease of particle diameter. The effect of an increase in viscosity (in Ohnesorge number, Eq. (9)) is to increase the diameter size, the effect of ultrasound frequency (which is present in all the dimensionless numbers and in the multiplying factor) is proportional to the power ($-0.66 + \Pi_2 + \Pi_3 - 2\Pi_4 = -0.277$) therefore, higher the frequency, smaller the particles (accordingly with Lang's equation).

3.2. Process intensification

The atomization is a fundamental step in a number of industrial applications. Often, it is the step which requires the most of the volumetric energy in the plant, since a lot of surface area has to be created (a flow rate of fluid has to be transformed in minute droplets, with a huge surface area). An estimation of the energy required for the atomization of a given flow rate (10 GPM gallon per minute = 6.3×10^{-4} m^3 s^{-1}) to 70 μm droplets is in [19]. The use of the two fluid technology (atomization of a liquid assisted by a compressed gas) requires a volumetric power supply which is roughly 41 MJ m^{-3} (6 of which being required to pump the liquid at a pressure of 0.35 MPa, the remaining 35 to compress air at the same pressure, the air flow rate is taken as 180 SCFM (Standard Cubic Foot per Minute) = 0.085 N m^3 s^{-1}). The use of the centrifugal atomizer (in which the droplet were obtained because of the fast rotation of the feed) requires 33 MJ m^{-3} (3.5 of which being required to pump the liquid at a pressure of 0.21 MPa, the remaining 29.5 to operate the centrifugal atomizer rotating at 9000 rpm). The use of the pressure nozzle (in which the droplet were created by passing the pressurized feed into an orifice) requires 12 MJ m^{-3} (all of which being required to pump the liquid at a pressure of 8.3 MPa). Similar data (energy requirements: two fluids > centrifugal atomizer > pressure nozzle) are reported elsewhere in technical literature [20].

In Fig. 6 the volumetric power supply for the runs carried out in the present study (which can be easily calculated with the data from Table 1, being the ratio $P/\dot{V}$) were reported versus the volumetric flow rate. It is evident that the increase in volumetric flow rate causes the volumetric power supply to decreases a lot, and the higher flow rate investigated (of the order of 6×10^{-9} m^3 s^{-1}) requires a volumetric power supply around 10 MJ m^{-3}. Furthermore, the data seem to present an asymptotical behavior. Thus, working at the highest flow rate allowed by the laboratory system, very low volumetric power supply is required, comparable with the

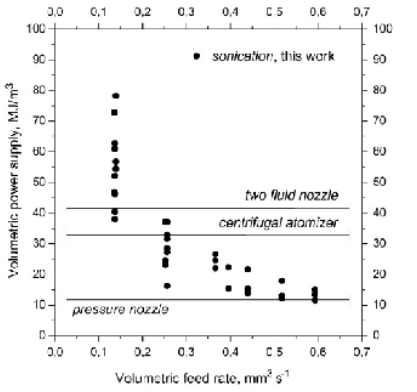

Fig. 6. Volumetric power supply vs. volumetric feed rate for the experiments performed, in comparison with the volumetric power supply for different atomization techniques [19].

lowest value realized on plant scale using conventional techniques. Since, usually, the lab scale requires specific energy higher than the plant scale, the ultrasonic assisted atomization is confirmed to be a very promising technique in the intensification of industrial processes which includes an atomization step.

4. Conclusions

In this work, the ultrasonic atomization of alginate solutions, a natural polymer with a great potential in pharmaceutical and nutraceutical productions, has been carried out on the laboratory scale. Process parameters have been changed (alginate concentration, volumetric flow rate, power delivered), and the resulting particle diameters have been measured. Correlations available in literature have been tested and, since they were found not able to reproduce observed data, the parameters regression was performed, along with a careful statistical data analysis. Finally, the energetic of the process was analyzed and compared with other atomization techniques.

The results of this work could be summarized as follows:

- a method to obtain and to characterize small alginate particles has been pointed out;
- the process parameters have been successfully correlated to the particle diameters;
- the ultrasonic atomization has been confirmed to be a process with a low volumetric energy request, being thus an efficient tool in process intensification.

Appendix A. Nomenclature

A_{act}	surface of ultrasonic actuator (m^2)
Am	sound wave amplitude (m)
c	concentration alginate in water (% w/w)
c^*	reference alginate concentration 1.3%
C	speed of sound ($m\,s^{-1}$)
$\langle D\rangle$	average diameter (μm)
D_A	Correlation A particle diameter (μm)
$\langle D_A\rangle$	average diameter (μm)
D_B	Correlation B particle diameter (μm)
$\langle D_B\rangle$	average diameter (μm)
D_L	Lang particle diameter (μm)
f	ultrasonic frequency (kHz)
I	power surface intensity, P/A ($W\,m^{-2}$)
in	intensity number
K	consistency index ($Pa\,s^n$)
L_{act}	length of the ultrasonic actuator (m)
n	flow index
Oh	Ohnesorge number
P	power (W)
$P_{1\ldots7}$	parameters
R	radius of circular tube (m)
R_{act}	radius of the ultrasonic actuator (m)
R^2	Pearson coefficient
SD	standard deviation
SSE	Sum of Square Errors
$\dot{V}$	flow rate ($m^3\,s^{-1}$)
VAR	variance, experimental data (μm^2)
VAR_A	variance, Correlation A (μm^2)
VAR_B	variance, Correlation B (μm^2)
We	Weber number

Greek symbols

$\dot{\gamma}$	shear rate (s^{-1})
$\dot{\gamma}_W$	shear rate at wall (s^{-1})
η	viscosity (Pa s)
$\Pi_{1\ldots4}$	parameters
ρ^*	alginate–water solution density ($kg\,m^{-3}$)
ρ_0	water density ($kg\,m^{-3}$)
σ^*	alginate–water surface tension ($m\,N\,m^{-1}$)
σ_0	water surface tension ($m\,N\,m^{-1}$)

References

[1] J.M. Coulson, J.F. Richardson's Chemical Engineering—Particle Technology and Separation Processes, Butterworth-Heinemann, Woburn MA, 5th ed., 2002, vol. 2, Section 2b2 Process Intensification.

[2] R. Rajan, A.B. Pandit, Correlations to predict droplet size in ultrasonic atomization, Ultrasonics 31 (2001) 235–255.

[3] M. George, T.E. Abraham, Polyionic hydrocolloids for the intestinal delivery of protein drugs: alginate and chitosan – a review, J. Controlled Release 114 (2006) 1–14.

[4] S. Martins, B. Sarmento, F.R. Souto, D.C. Ferreira, Insulin loaded alginate microspheres for oral delivery—effect of polysaccharide reinforcement on physicochemical properties and release profile, Carbohydr. Polym. 69 (2007) 725–731.

[5] V.R. Babu, M. Sairam, K.M. Hosamani, T.M. Aminabhavi, Preparation of sodium alginate–methylcellulose blend microspheres for controlled release of nifedipine, Carbohydr. Polym. 69 (2007) 241–250.

[6] M. Rajaonarivony, C. Vauthier, G. Couarraze, F. Puisieux, P. Couvreur, Development of a new drug carrier made from alginate, J. Pharm. Sci. 82 (9) (1993) 912–917.

[7] M. Leonard, M. Rastello De Boisseson, P. Hubert, F. Dalencon, E. Dellacherie, Hydrophobically modified alginate hydrogels as protein carriers with specific controlled release properties, J. Controlled Release 98 (2004) 395–405.

[8] P. Leerunyakhiwong, K. Nooruin, N. Jongaroonngamsang, P. Rojsitthisak, U. Nimmannit, Preparation of alginate nanocapsules containing turmeric oil, Carbohydr. Polym. 74 (2008) 209–214.

[9] W. Klaypradit, Y.W. Huang, Fish oil encapsulation with chitosan using ultrasonic atomizer, LWT 41 (2008) 1133–1139.

[10] J.A. Ko, S.Y. Koo, H.J. Park, Effects of alginate microencapsulation on the fibrinolytic activity of fermented soybean paste (Cheonggukjang) extract, Food Chem. 111 (2008) 921–924.

[11] S.K. Bajpai, R. Tankhiwale, Investigation of water uptake behavior and stability of calcium alginate/chitosan bi-polymeric beads: Part-I, React. Funct. Polym. 66 (2006) 645–658.

[12] C. Afonso, L. Ferreira, Helder Vila Real, A.J. Alfaia, M.H.L. Ribeiro, High pressure and temperature combination with nattokinase hydrolysis by nattokinase Ca-alginate beads in grapefruit juice processing: bitterness and microbial reduction, Abs/J. Biotechnol. 131S (2007) S263–S265.

[13] M.F. Malone, J.A.M. Appelqvist, Gelled emulsion particles for the controlled release of lipophilic volatiles during eating, J. Controlled Release 90 (2003) 227–241.

[14] H. Brandenberger, F. Widmer, A new multinozzle encapsulation/immobilisation system to produce uniform beads of alginate, J. Biotechnol. 63 (1998) 73–80.

[15] V.G. Babak, E.A. Skotnikova, I.G. Lukina, S. Pelletier, P. Hubert, E. Dellacherie, Hydrophobically associating alginate derivatives: surface tension properties of their mixed aqueous solutions with oppositely charged surfactants, J. Colloid Interface Sci. 225 (2000) 505–510.

[16] R.B. Bird, W.E. Stewart, E.N. Lightfoot, Transport Phenomena, 2nd ed., John Wiley & Sons, New York, 2002, pp. 241–243.

[17] R.J. Lang, Ultrasonic atomization of liquids, J. Acoust. Soc. Am. 34 (1962) 6–8.

[18] M. Grassi, C. Grassi, R. Lapasin, I. Colombo, Understanding Drug Release and Absorption Mechanisms, CRC Press, Boca Raton, USA, 2007, p. 25.

[19] http://www.spraydrysys.com/spray-dryers/spray-drying-technology/spray-drying-atomization.htm.

[20] I. Pilkova, L.X. Huang, A.S. Mujumdar, Industrial spray drying systems, in: A.S. Mujumdar (Ed.), Handbook of Industrial Drying, 3rd ed., CRC Press, Boca Raton, USA, 2006, p. 225 (Chapter 10).

Bibliografia

1. R. Rajan and A.B. Pandit, Correlations to predict droplet size in ultrasonic atomization, *Ultrasonics*, **31** 235-255 (2001).
2. S. H. Yuk, pH sensitive drug delivery system using O/W emulsion, *Journal of Controlled Release*, **37** 69 – 74 (1995).
3. A.P. Rodrigues et al., Production and characterisation of alginate microparticles incorporating *Aeromonas Hydrophila* designed for fish oral vaccination, *Process Biochemistry* **41** 638 – 643 (2006).
4. V. R. Babu et al., Preparation of sodium alginate – methylcelluse blend microspheres for controlled release of nifedipine, *Carbohydrate Polymers* **69** 241 – 250 (2007).
5. S.K. Bajpai and R. Tankhiwale, Investigation of water uptake behavior and stability of calcium alginate/chitosan bi – polymeric beads: Part - 1, *Reactive & Functional Polymers* **66** 645 – 658 (2006).
6. S.M. Jay and W.M. Saltzman, Controlled delivery of VEGF via modulation of alginate microparticle ionic crosslinking, *Journal of Controlled Release* **134** 26 – 34 (2009).
7. P. Lertsutthiwong et al., Preparation of alginate nanocapsules containing turmeric oil, *Carbohydrate Polymers* **74** 209 – 214 (2008).
8. Q. Ain et al., Alginate – based oral drug delivery system for tubercolosis: pharmacokinetics and therapeutic effects, *Journal of Antimicrobial Chemotherapy* **51** 931 – 938 (2003).
9. S. Martins et al., Insulin - loaded alginate microspheres for orl delivery – Effect of polysaccharide reinforcement on physicochemical properties and release profile, *Carbohydrate Polymers* **69** 725 – 731 (2007).
10. J. Tu et al., Alginate microparticles prepared by spray – coagulation method: Preparation, drug loading and release characterization, *International Journal of Pharmaceutics* **303** 171 – 181 (2005).
11. K. Mladenovska et al., Colon specific delivery of 5 – aminosalicylic acid from chitosan – Ca – alginate microparticles, *International Journal of Pharmaceutics* **342** 124 – 136 (2007).

12. C. Cavallari et al., Thermal and Fractal Analysis of Diclofenac/Gelucire 50/13Microparticles Obtained by Ultrasound – Assisted Atomization, *Journal of Pharmaceutical Sciences* **94** (5) 1124 – 1134 (2005).

13. S. Freitas et al., Ultrasonic atomization into reduced pressure atmosphere – envisaging aseptic spray – drying for microencapsulation, *Journal of Controlled Release* **95** 185- 195 (2004).

14. W. Klaypradit and Y.W. Huang, Fish oil encapsulation with chitosan using ultrasonic atomization, *LWT* **41** 1133 – 1139 (2008).

15. B. Avvaru et al., Ultrasonic atomization: Effect of liquid phase properties, *Ultrasonics* **44** 146 – 158 (2006).

16. H. Brandenberger and F. Widmer, A new multinozzle encapsulation: immobilisation system to produce uniform beads of alginate, *Journal of Biotechnology*, **63** (1998) 73–80.

17. V.G. Babak, Associating Alginate Derivatives: Surface Tension Properties of Their Mixed Aqueous Solutions with Oppositely Charged Surfactants, *Journal Of Colloind and Interface Science*, **225** (2000) 505-510.

18. http://www.accessdata.fda.gov/scripts/fcn/fcnDetailNavigation.cfm?rpt=scogsListing&id=44.

19. http://www.dow.com/PublishedLiterature/dh_0035/0901b803800355ea.pdf?filepath=methocel/pdfs/noreg/198-02069.pdf&fromPage=GetDoc

20. R.J. Lang, Ultrasonic atomization of liquids, Journal of Acoustical Society of America, **34** 6-8 (1962).

21. T. Mochida, Proc. ICLASS – 78, 1978, p. 193.

22. P. Walzel, Liquid atomization, *International Chemical Engineering*, **33** (1) 46 – 60 (1993).

23. Cuofano C., Reticolazione di geli a base di alginato – Pluronico F 127 con rame bivalente, Tesi di laurea in Ingegneria Chimica, Università degli Studi di Salerno (2009).